Micro and Nano Systems Letters

LETTER

Open Access

Fabrication of surface-functionalized PUA composites to achieve superhydrophobicity

Tian-Feng Hou[1], Arunkumar Shanmugasundaram[1], Bui Quoc Huy Nguyen[1] and Dong-Weon Lee[1,2*]

Abstract

Herein, we present a facile fabrication method to prepare the optically transparent, flexible and self-cleanable poly(urethane acrylate) (PUA) superhydrophobic film. The low surface energy siloxane functionalization on the thermally activated μ-patterned PUA/graphene oxide composite (S-PG) was found to be a successful strategy to modify the PUA intrinsic hydrophilicity into superhydrophobic nature. The S-PG film (with GO content of 0.1 wt%) repeatedly showed the water contact angle (WCA) of 149.82 ± 1° with excellent self-cleaning property. Further, the fabricated film exhibited high optical transparency (80%) in the 400–800 nm wavelength region. Finally, the practical applicability of the fabricated S-PG film was demonstrated by using the film as a protective layer for solar panel module. The power conversion efficiency (PCE) of the solar module with and without S-PG superhydrophobic film was found to be 5.98% and 5.82%, respectively. The enhancement in the PCE performance of the solar module is attributed to the excellent optical transparent and less light reflecting nature of the proposed film.

Keywords: Siloxane functionalization, PUA, Polydimethylsiloxane (PDMS), Chemical vapor deposition (CVD)

Introduction

A surface that exhibits a WCA more than 150° with a sliding angle (SA) less than 10° is commonly called superhydrophobic surface [1, 2]. Such surface is always self-cleaned by the enrolling water droplet and received significant attention in several applications, such as antifouling, self-cleaning, anti-friction, oil/water separation. The optically transparent superhydrophobic film has been used as a protective layer in numerous electronic devices, solar cell panels, safety goggles, construction, stain-resistant textiles, microfluidics, biomedical devices, energy harvesting, aerospace, marine and automobiles industries [3–5]. Several years of research on superhydrophobic film have provided key understanding on the control parameters and material tailoring techniques [4, 6, 7]. Among them, efforts have demonstrated that a combination of microscale roughness in synthetic materials together with low surface energy could greatly improve the superhydrophobic nature of the material [7–9]. Over the years, several polymers, such as polyethylene terephthalate (PET) [10–12], poly(methyl methacrylate) (PMMA) [13, 14], and polydimethylsiloxane (PDMS) [15–17] based superhydrophobic films have been reported by employing those above-mentioned techniques. Although PUA has several attracting properties like biocompatibility, high deformability and excellent impact strength, UV-curability at ambient atmosphere and high transparency in visible light region, there is no report on the PUA based superhydrophobic film owing to its intrinsic hydrophilicity. The practical applicability of PUA as a superhydrophobic surface is met with limited success owing to its high surface energy. The intrinsic hydrophilicity of PUA can be modified by functionalizing the low surface energy materials by covalent surface functionalization. However, the chemical inertness of PUA makes its surface unfeasible for functionalizing with other reactive groups. Therefore, developing an effective and efficient method to create active functional groups on PUA surface is crucial for making its surface suitable for superhydrophobic applications.

Herein, we demonstrate in detail our successful attempt to fabricate the PUA based superhydrophobic film by employing the microarchitectures and surface

*Correspondence: mems@jnu.ac.kr
[1] MEMS and Nanotechnology Laboratory, School of Mechanical Engineering, Chonnam National University, Gwangju 61186, Republic of Korea
Full list of author information is available at the end of the article

modification with low surface energy siloxane. Graphene oxide (GO) was incorporated into PUA to create several active functional groups on the inert PUA surface. The active functional groups play an important role during surface functionalization with low surface energy materials such as siloxane. In addition, the active functional groups improve the chemical bonding between the PUA and low surface energy siloxane [18]. The fabricated film was characterized in detail by field emission scanning electron microscopy (FESEM) and Fourier transform infrared spectroscopy (FTIR) for its morphological and chemical analysis, respectively. The obtained results are consistent and confirmed the successful formation of the siloxane functionalized PUA and GO composite (S-PG) superhydrophobic film. Finally, the fabricated film was used as a protection layer for the solar module to demonstrate the practical applicability of the fabricated film.

Materials and methods

Fabrication of the μ-patterned SU-8 mold

In a typical fabrication process, a 4 inch Si wafer was cleaned with standard piranha solution (H_2SO_4:H_2O_2 (2:1) for 20 min), deionized water and then dried with nitrogen stream. Subsequently, the Si wafer was dehydrated on the hotplate at 150 °C for 30 min. Next, 4 mL of SU-8 (Micro Chem Corp., SU-8, 3010) negative photoresist was spin-coated on the Si wafer at 300 rpm for 5 s, followed by 800 rpm for another 30 s to obtain a ~ 20 μm thick resist layer. Then the film was exposed to ultraviolet (UV) light for transferring the mask pattern to the SU-8 layer. Subsequently, the SU-8 coated Si wafer was soft baked on a hotplate at 65 °C for 1 min and 95 °C for 10 min. Finally, the photoresist layer was developed by immersion technique in a developer solution (Micro Chem's SU-8 Developer) for 5 min to release the μ-pillar structure (Scheme 1a).

Fabrication of the negative PDMS mold

The PDMS (Sylgard 184) base and thermal curing agent (containing a Pt-based catalyst) were purchased from Dow Corning Corporation (Wiesbaden, Germany). The negative mold of PDMS was made by a thermal casting method. The PDMS base and the curing agent were mixed with the weight ratio of 10:1 and then degassed in vacuum for 1 h. The mixture was then poured onto μ-patterned SU-8 mold (fabricated by photolithography process) and cured on the hotplate for 4 h at 80 °C (Scheme 1b). The cross-linking polymerization occurred in the thermal casting process as shown in Additional file 1: Fig. S1.

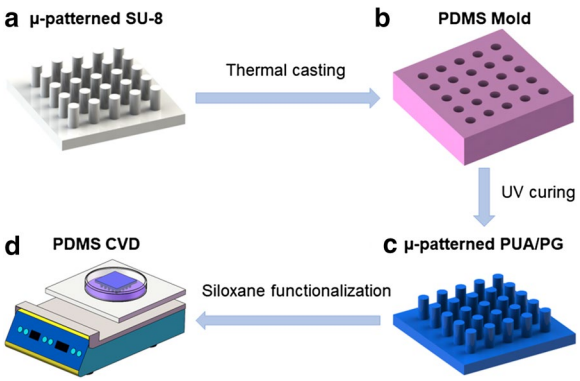

Scheme 1 The fabrication process for superhydrophobic film of functionalized GO incorporated PUA composite (S-PG)

Fabrication of the μ-patterned PG film

The PUA + GO (PG) hybrid composite μ-patterned was fabricated by the mold transfer technique. Firstly, 0.1 wt% (1 mg/1 mL) of GO and 99.9% of PUA were ultrasonically dispersed for 30 min. Then, the mixture was heated to 80 °C in the programable furnace and maintained at that temperature for 2 h. Subsequently, the PG was poured into the negative PDMS mold. Then, a flexible and transparent poly (ethylene terephthalate) (PET) supporting film was attached to the mixture of PG. Next, a uniform PG layer was formed on the PDMS mold by mild rolling a roller on top surface of the PET film. Finally, the PG coated PDMS mold was exposed to UV light with an energy of ~ 1620 mJ/cm^2 for 10 h. After the UV treatment, the μ-patterned PG film was removed from the PDMS mold (Scheme 1c).

Fabrication of siloxane functionalized μ-patterned PG film

The low surface energy siloxane was functionalized on the thermally activated PG through PDMS chemical vapor deposition (CVD). In a typical fabrication process, the prepared μ-patterned PG film was attached to the glassware in an upside-down position and placed above the pre-polymer of PDMS coated Si wafer. The PDMS CVD was performed on a hotplate at 285 °C at various time to prepare the siloxane functionalized μ-patterned PG film. After the CVD, the prepared siloxane functionalized μ-patterned PG film was ultrasonically cleaned with ethanol by the ultrasonication for 30 min to remove the unreacted siloxane from the surface of the μ-patterned PG film (Scheme 1d).

Power conversion efficiency of solar cell

The fabricated S-PG film was used as protection layer for the solar cell. The current–voltage (J–V) curves of the solar cell with and without the protection layer were characterized by a class AAA solar simulator

(WXS-155S-L2, WACOM, and Japan) with the condition of AM 1.5G, 100 mW/cm^2 at room temperature. The PCE of the solar cells with and without the protection layer were calculated using the following equation:

$$PCE = \frac{P_{out}}{P_{in}} = \frac{J_{SC} V_{OC} FF}{P_{in}}$$

where, P_{out} and P_{in} is the output and input power of the cell, FF is the fill factor, and J_{SC} and V_{OC} are the short-circuit current density and open-circuit voltage respectively. The fill factor was calculated by the following equation.

$$FF = \frac{J_{MP} V_{MP}}{J_{SC} V_{OC}}$$

where, J_{MP} and V_{MP} are the current density and voltage of the cell at maximum power respectively.

Results and discussion

Morphology of the fabricated S-PG superhydrophobic film, was observed by the FESEM analysis. The low magnified FESEM image shows several μ-pillars with uniform shape and size and microscale roughness of the fabricated film (Fig. 1a, b). The dimension of the fabricated film was ~ 20 μm in diameter, ~ 20 μm in height and 70 μm in pillar space, respectively. To further identify the important of GO for the functionalization of the siloxane group on the PUA surface, siloxane functionalization was also performed with the pristine μ-pillar PUA film. Additional file 1: Figs. S2 and S3 show the elemental mapping of the siloxane functionalized μ-pillar PUA (S-PUA) and S-PG film. The elemental clearly reveals the uniform distribution of carbon, nitrogen, oxygen and silicon. The elemental mapping of pristine PUA does not showed any silicon distribution on the PUA surface. Whereas, the elemental mapping of PG film showed the presence of silicon indicating the successful chemical functionalization of siloxane group on the surface of PG.

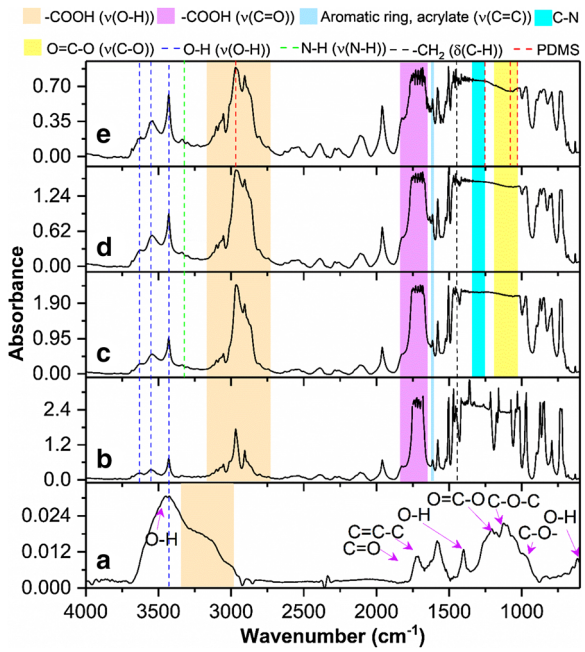

Fig. 2 The Fourier transform infrared (FTIR) spectra of (a) GO, (b) PET, (c) PUA film, (d) GO incorporated PUA composite film (PG) and (e) siloxane functionalized GO incorporated PUA composite film (S-PG)

Further, the materials were characterized in detail by different techniques and the obtained results confirm the successful formation of the siloxane functionalized μ-patterned PUA film. The functional group on the surface of the prepared films was analysis using FTIR spectra as shown in Fig. 2. The FTIR spectrum of GO (Fig. 2a) showed an intense peak at 3445 cm^{-1} and other lower intensity band at 3300–2925 cm^{-1} and peaks at 1723, 1583, 1400, 1206, 1124, 836 and 616 cm^{-1}. These peaks corresponded to the –OH groups, the stretching of –OH and C=O in carboxylic acid groups, the aromatic ring

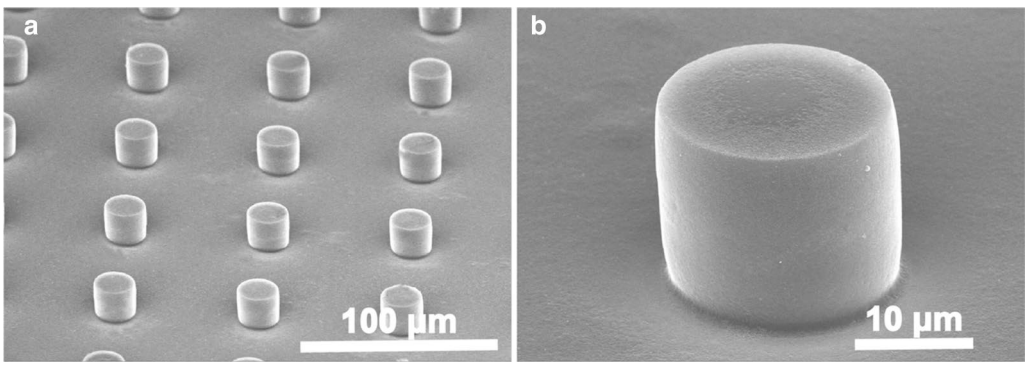

Fig. 1 Field emission scanning electron microscope (FESEM) images of the siloxane functionalized μ-patterned GO incorporated PUA hybrid superhydrophobic film at (**a**) lower and (**b**) higher magnifications

stretching, –OH bending in phenol, C–O stretching in phenol, C–O stretching in C–O–C, epoxy stretching and OH out-of-plan bending, respectively. The bands and functional groups of PET (Fig. 2b) were confirmed corresponding to the commercial PET film reported in the Ref. [19]. After the PUA was deposited on the PET film, peaks and bands at 3337, 1850–1650 and 1250–1100 cm^{-1}, assigned to the N–H stretching of aliphatic primary amine, C=O stretching vibration of urethane bond and C–O stretching of aliphatic, respectively (Fig. 2c). It indicates the formation of urethane linkages. In addition, even though there was a band at 1643–1614 cm^{-1}, it was attributed to the stretch vibration of C=C due to the PET film, further indicating that the PUA was fully cured. With the addition of the GO, the intensity of the peaks, including –OH (3624, 3541, 3429 cm^{-1}), –COOH (3102–2806, 2300–2000 cm^{-1}), C=O (1850–1650 cm^{-1}), were significantly increased (Fig. 2d). With the siloxane functionalization via PDMS CVD, the S-PG (Fig. 2e) showed C–H antisymmetric stretching ($\nu_{(as)}$(CH)) and C–H symmetric stretching ($\nu_{(s)}$ (CH)) peaks of $Si(CH_3)_2$ groups at 2970.4 cm^{-1} and 1257.6 cm^{-1}, respectively [20, 21]. In addition, the bands were observed between 1000 and 1100 cm^{-1} representing the stretching of Si–O–Si (ν(Si–O–Si)), which were characteristic of a PDMS polymeric network. Characteristic peaks at 1014.6 cm^{-1} and 1072.4 cm^{-1} were associated with ν(Si–O–Si) peaks in the cyclic-D_3/D_4 and linear siloxanes, respectively [22]. It indicates that the siloxane functionalized surface has the same chemical properties as the PDMS elastomer.

The water contact angle (WCA) measurement was performed to confirm the successful hydrophobization of the PUA surface by PDMS CVD. The volume of the water droplet used for the analysis was ~5 µL and the distance between the sample surface and the water droplet is 10 mm. As shown in Fig. 3, the WCAs of the S-PG films increased with increasing the pillar distance and reached the maximum value for the µ-pillar pattern with space of 70 µm and then decreased. The WCA was found to be 149.82 ± 1°. It indicates that the wetting state was changed from Cassie–Baxter's state to Wenzel's state at the critical µ-pillar space of 70 µm for the as fabricated film. The water advancing contact angle (WACA), water receding contact angle (WRCA) and sliding angle (SA) of S-PG film were further measured. Additional file 1: Fig. S4 shows the WACA, WRCA and SA of the fabricated S-PG film at different µ-pillar distance. The WACA of the fabricated film was found to be 143.86 ± 0.45° when the pillar distance was 40 µm. Then, it was increased with increasing pillar distance, reached the value of 155.5 ± 0.3° for the film with pillar distance of 70 µm and saturated with further increasing the pillar distance. The WRCA of the fabricated film at 40 µm was ~ 121.25 ± 0.82° and attained maximum value of 143.4 ± 0.6° at 70 µm, then decreased to 91.02 ± 1.62° when the pillar distance increased to 90 µm and above. The SA of the as prepared film rapidly increased starting from the pillar distance increased from 80 to 90 µm and attained the maximum value of 60.3 ± 0.6° and then saturated. Finally, the SA showed a slightly increased until the pillar distance increased to 120 µm. This could be due to lack of formation of air pockets at pitch values ranging from 90 to 120 µm. Furthermore, to effectively demonstrate the role of µ-pillars on the improved superhydrophobicity, we have prepared the flat surface PG (F-PG) film and functionalized with the siloxane using the same fabrication method as described in the previous section. Additional file 1: Fig. S5 shows the WCA of the siloxane functionalized flat surface PG (S-F-PG) film, which was found to be ~ 97°.

To demonstrate the practical applicability of the proposed transparent superhydrophobic film, the as fabricated SP-G film was used as a protection layer for the home-made solar cell module (insert of Fig. 4). A piece

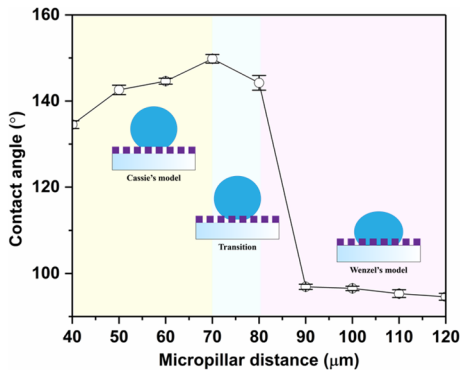

Fig. 3 The static water contact angle (WCA) of the siloxane functionalized GO incorporated PUA (S-PG) composite film as a function of µ-pillar distance

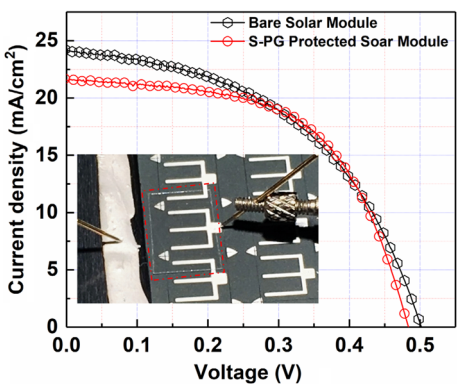

Fig. 4 J–V characteristics of the solar cell module with and without siloxane functionalized GO incorporated PUA composite film (S-PG) superhydrophobic film with µ-pillar distance of 70 µm

of the as-fabricated S-PG film was cut to cover one solar cell of the module as shown in the red dashed box. The high transmittance of the film was confirmed by the clear appearance of the underneath solar cell module. The photovoltaic performance of a solar cell module with and without the as fabricated S-PG as protection layer was evaluated. The current–voltage (J–V) curve were shown in Fig. 4 and the calculated PCE values were shown in Table 1. The PCE value of S-PG superhydrophobic film protected solar module was ~5.98%, which showed improved PCE performance comparing to that of bare solar cell module (5.82%).

The enhanced performance of the S-PG-protected solar cell module is attributed to the high optical transparency and less light reflecting nature of the proposed film. The high transmittance of the film was confirmed by the clear appearance of the underneath solar cell module. The high transparency and less reflecting nature of the proposed superhydrophobic film was confirmed by the ultraviolet diffused reflectance spectroscopy (UV-DRS) analysis. The UV-DRS spectrum of the fabricated S-PG film recorded in the % transmittance and reflectance mode between 400 and 700 nm are shown in Additional file 1: Fig. S6. The fabricated film was showed the optical transparency more than 80% and reflectance lower than 10% in the visible light region. The UV-DRS analysis clearly reveals the high optical transparency and low reflectance of the proposed film. The improved PCE performance of the S-PG protected solar module could be explained based on the following lines. The μ-patterned film has good light trapping effect made by the periodic vertically aligned micropillar on the surface, thus decreasing the light reflectance. As shown in Scheme 2a, when light incidents the bare cell, a large fraction of light is directly absorbed by the solar cell while a small fraction of light is inevitably reflected. However, since the high transmittance of the S-PG film, a large fraction of the light transmits from air into the S-PG film reaching the solar cell while a small fraction of the light is reflected onto the neighboring μ-pillars when the light incident at different angles (Scheme 2b). Then, the reflected light enters the μ-patterned film again and most of them is transmitted to the underneath solar cell, which improves the usage of the light and thus increasing the total absorbance of the solar cell. Thus, the solar cell covered with the μ-patterned film would absorb more light than the bare solar cell. The increase of the PCE value with the microstructure patterned protection film was also recently reported [23–26].

Table 1 Photovoltaic characteristics of the solar cell module covered with and without fabricated siloxane functionalized GO incorporated PUA composite (S-PG) superhydrophobic film with μ-pillar distance of 70 μm

Solar cell module	J_{sc} (mA cm^{-2})	V_{oc} (V)	FF	PCE (%)
Bare	24.15	0.50	0.48	5.82
S-PG protected	21.56	0.48	0.57	5.98

Conclusions

In conclusions, we have fabricated optically transparent, flexible and self-cleanable PUA superhydrophobic film by siloxane functionalization through PDMS CVD. The fabricated siloxane functionalized GO incorporated PUA composite film showed high WCA of 149.82 ± 1° with an optical transmittance of more than 80% in the 400–800 nm wavelength region. Final the fabricated the superhydrophobic film was used as protection layer for the home-made solar cell module. The solar module protected with the fabricated superhydrophobic film showed improved performance owing to the high optical transparency and less light reflecting nature of the material.

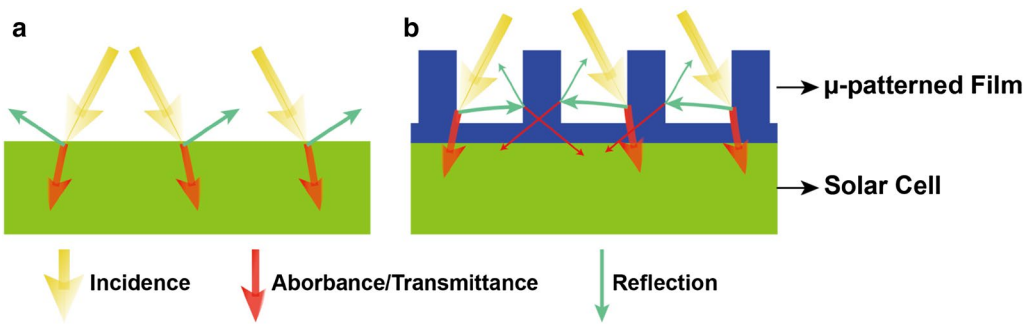

Scheme 2 Schematics of light incidents the **a** bare solar cell and **b** μ-patterned high transmittance film protected solar cell as well as its trapping effect

Supplementary information

Supplementary information accompanies this paper at https://doi.org/10.1186/s40486-019-0090-9.

Additional file 1: Fig. S1. The PDMS cross-linking polymerization reaction. **Fig. S2.** Elemental analysis of the fabricated μ-patterned siloxane functionalized PUA (S-PUA). (a) Electron micrograph of μ-pillar top surface, elemental mapping of (b) carbon, (c) nitrogen and (d) oxygen. **Fig. S3.** Elemental analysis of the fabricated μ-patterned siloxane functionalized PG (S-PG). (a) electron micrograph of μ-pillar top surface, elemental mapping of (b) carbon, (c) nitrogen, (d) oxygen and (e) silicon. **Fig. S4.** The water advancing contact angle (WACA), water receding contact angle (WRCA) and sliding angle (SA) of the siloxane functionalized GO incorporated PUA composite (S-PG) film as a function of μ-pillar distance, (n = 5, mean ± standard deviation). **Fig. S5.** Photograph of a water droplet on the surface of the siloxane functionalized flat PG (S-F-PG). **Fig. S6.** The UV-DRS spectra of the fabricated siloxane functionalized-μ-patterned PG (S-PG) film.

Acknowledgements
Authors are grateful to the National Research Foundation of Korea for the funds received.

Authors' contributions
TFH designed the research, discussed the results with AS and DWL also contributed to writing the manuscript with DWL. NBQH fabricated SU-8 mold. All authors read and approved the final manuscript.

Funding
This work was supported by National Research Foundation of Korea (NRF) funded by the Korean government (MSIP) (No. 2015R1A4A1041746).

Competing interests
The authors declare that they have no competing interests.

Author details
[1] MEMS and Nanotechnology Laboratory, School of Mechanical Engineering, Chonnam National University, Gwangju 61186, Republic of Korea. [2] Center for Next-generation Sensor Research and Development, Chonnam National University, Gwangju 61186, Republic of Korea.

Received: 4 June 2019 Accepted: 22 August 2019
Published online: 30 August 2019

References

1. Quan YY, Zhang LZ, Qi RH, Cai RR (2016) Self-cleaning of surfaces: the role of surface wettability and dust types. Sci Rep 6:38239
2. Li H, Zhao Y, Yuan X (2013) Facile preparation of superhydrophobic coating by spraying a fluorinated acrylic random copolymer micelle solution. Soft Matter 9(4):1005–1009
3. Sahoo B, Yoon K, Seo J, Lee T (2018) Chemical and physical pathways for fabricating flexible superamphiphobic surfaces with high transparency. Coat 8(2):47
4. Das S, Kumar S, Samal SK, Mohanty S, Nayak SK (2018) A review on superhydrophobic polymer nanocoatings: recent development and applications. Ind Eng Chem Res 57(8):2727–2745
5. Zhang Y, Dong B, Wang S, Zhao L, Wan GL, Wang E (2017) Mechanically robust, thermally stable, highly transparent superhydrophobic coating with low-temperature sol–gel process. RSC Adv 7(75):47357–47365
6. Nosonovsky M, Bhushan B (2009) Superhydrophobic surfaces and emerging applications: non-adhesion, energy, green enineering. Curr Opin Colloid Interface Sci 14(4):270–280
7. Ragesh P, Ganesh VA, Nair SV, Nair AS (2014) A review on 'self-cleaning and multifunctional materials'. J Mater Chem A 2(36):14773–14797
8. Kumar KSS, Kumar V, Nair CPR (2014) Bulk superhydrophobic materials: a facile and efficient approach to access superhydrophobicity by silane and urethane chemistries. J Mater Chem A 2(37):15502–15508
9. Xue CH, Jia ST, Zhang J, Ma JZ (2010) Large-area fabrication of superhydrophobic surfaces for practical applications: an overview. Sci Technol Adv Mater 11(3):033002
10. Hikita M, Tanaka K, Nakamura T, Kajiyama T, Takahara A (2005) Super-liquid-repellent surfaces prepared by colloidal silica nanoparticles covered with fluoroalkyl groups. Langmuir 21(16):7299–7302
11. Tadanaga K, Kitamuro K, Matsuda A, Minami T (2003) Formation of superhydrophobic alumina coating films with high transparency on polymer substrates by the sol–gel method. J Sol–Gel Sci Technol 26(1–3):705–708
12. Teshima K, Sugimura H, Inoue Y, Takai O, Takano A (2005) Transparent ultra water-repellent poly (ethylene terephthalate) substrates fabricated by oxygen plasma treatment and subsequent hydrophobic coating. Appl Surf Sci 244(1–4):619–622
13. Kontziampasis D, Boulousis G, Smyrnakis A, Ellinas K, Tserepi A, Gogolides E (2014) Biomimetic, antireflective, superhydrophobic and oleophobic PMMA and PMMA-coated glass surfaces fabricated by plasma processing. Microelectron Eng 121:33–38
14. Han Z, Wang Z, Li B, Feng X, Jiao Z, Zhang J, Zhao J, Niu S, Ren L (2019) Flexible self-cleaning broadband antireflective film inspired by the transparent cicada wings. ACS Appl Mater Interfaces 11(18):17019–17027. https://doi.org/10.1021/acsami.9b01948
15. Im M, Im H, Lee JH, Yoon JB, Choi YK (2010) A robust superhydrophobic and superoleophobic surface with inverse-trapezoidal microstructures on a large transparent flexible substrate. Soft Matter 6(7):1401–1404
16. Dufour R, Harnois M, Coffinier Y, Thomy V, Boukherroub R, Senez V (2010) Engineering sticky superomniphobic surfaces on transparent and flexible PDMS substrate. Langmuir 26(22):17242–17247
17. Gong D, Long J, Jiang D, Fan P, Zhang H, Li L, Zhong M (2016) Robust and stable transparent superhydrophobic polydimethylsiloxane films by duplicating via a femtosecond laser-ablated template. ACS Appl Mater Interfaces 8(27):17511–17518
18. Nguyen BQH, Shanmugasundaram A, Hou TF, Park J, Lee DW (2019) Realizing the flexible and transparent highly-hydrophobic film through siloxane functionalized polyurethane-acrylate micro-pattern. Chem Eng J 373:68–77
19. Arahman N, Fahrina A, Amalia S, Sunarya R, Mulyati S (2017) Effect of PVP on the characteristic of modified membranes made from waste PET bottles for humic acid removal. F1000 Res. 6:668. https://doi.org/10.12688/f1000research.11501.2
20. O'Shaughnessy WS, Gao M, Gleason KK (2006) Initiated chemical vapor deposition of tri vinyl trimethylcyclotrisiloxane for biomaterial coatings. Langmuir 22(16):7021–7026
21. Lanzarotta A, Kelley CM (2016) Forensic analysis of human autopsy tissue for the presence of polydimethylsiloxane (Silicone) and volatile cyclic siloxanes using Macro FT-IR, FT-IR spectroscopic imaging and headspace GC–MS. J Forensic Sci 61(3):867–874
22. Jiao K, Zhou C, Becerra-Mora N, Fiske J, Kohli P (2016) Vapor-enhanced covalently bound ultra-thin films on oxidized surfaces for enhanced resolution imaging. J Mater Chem C 4(37):8634–8647
23. Myers JD, Cao W, Cassidy V, Eom SH, Zhou R, Yang L, You W, Xue J (2012) A universal optical approach to enhancing efficiency of organic-based photovoltaic devices. Energy Environ Sci 5(5):6900–6904
24. Cho C, Jeong S, Choi HJ, Shin N, Kim B, Jeaon EC, Lee JY (2015) Toward perfect light trapping in thin-film photovoltaic cells: full utilization of the dual characteristics of light. Adv Opt Mater 3(12):1697–1702
25. Liu D, Wang Q, Shen W, Wang D (2017) Self-cleaning antireflective coating with a hierarchical texture for light trapping in micromorph solar cells. J Mater Chem C 5(1):103–109
26. Tavakoli MM, Tsui KH, Zhang Q, He J, Yao Y, Li D, Fan Z (2015) Highly efficient flexible perovskite solar cells with antireflection and self-cleaning nanostructures. ACS Nano 9(10):10287–10295

Publisher's Note